Asian Journal of Chemistry; Vol. 32, No. 2 (2020), 401-407

ASIAN JOURNAL OF CHEMISTRY

https://doi.org/10.14233/ajchem.2020.22444

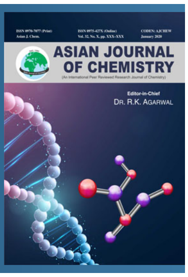

Molecular Geometry, NLO, MEP, HOMO-LUMO and Mulliken Charges of Substituted Piperidine Phenyl Hydrazines by Using Density Functional Theory

M. Dinesh Kumar[1,*], P. Rajesh[2], R. Priya Dharsini[2] and M. Ezhil Inban[3]

[1]Department of chemistry, Dr. N.G.P Arts and Science College (Autonomous), Coimbatore-641048, India
[2]Department of Chemistry, Government Arts College (Autonomous), Coimbatore-641018, India
[3]Department of Physics, Government Arts College (Autonomous), Coimbatore-641018, India

*Corresponding author: E-mail: dineshkumarm@drngpasc.ac.in

Received: 13 September 2019; *Accepted*: 29 October 2019; *Published online*: 30 December 2019; AJC-19734

The quantum chemical calculations of organic compounds *viz.* (*E*)-1-(2,6-*bis*(4-chlorophenyl)-3-ethylpiperidine-4-ylidene)-2-phenylhydrazine (3ECl), (*E*)-1-(2,6-*bis*(4-chlorophenyl)-3-methylpiperidine-4-ylidene)-2-phenylhydrazine (3MCl) and (*E*)-1-(2,6-*bis*(4-chlorophenyl)-3,5-dimethylpiperidine-4-ylidene)-2-phenylhydrazine (3,5-DMCl) have been performed by density functional theory (DFT) using B3LYP method with 6-311G (d,p) basis set. The electronic properties such as Frontier orbital and band gap energies have been calculated using DFT. Global reactivity descriptor has been computed to predict chemical stability and reactivity of the molecule. The chemical reactivity sites of compounds were predicted by mapping molecular electrostatic potential (MEP) surface over optimized geometries and comparing these with MEP map generated over crystal structures. The charge distribution of molecules predict by using Mulliken atomic charges. The non-linear optical property was predicted and interpreted the dipole moment (μ), polarizability (α) and hyperpolarizability (β) by using density functional theory.

Keywords: Mulliken charges, Molecular electrostatic potential, Non-linear optical property, Molecular geometry, Piperidin-4-ones.

INTRODUCTION

To analyze the biological activity of a molecule is a risk task today. Every molecule possesses some hidden properties based upon their electronic interactions with neighboring atoms and their biological activities are based on these interactions. Molecular docking is such type of a technique gives a basic idea of binding potency of a ligand with different selective proteins in a 3D arrangement [1]. It is an attractive platform to prospect rational drug design and discovery [2]. Another important emerging technique is computational quantum mechanical modeling [3]. *ab initio* DFT calculations are the most important method to determine the behaviour of a molecule on the basis of quantum chemical considerations [4]. From these calculations, several bond parameters like bond angle, bond length, and torsion angle can be calculated and also able to explore the activities of the selected molecules. Once we got an idea about the molecule then there is no hesitation to explain the nature of binding aspects.

Advances in organic chemistry were generally measured by the availability of simple and highly functionalized building blocks. It could be used in synthesizing larger molecules with tuning properties and its applications. Piperidine ring system plays a wide role in innumerable natural compounds and drugs. This variety of compounds manifests countless pharmacological properties [5]. Generally, substituted 4-piperidones are the modules of a many alkaloids which holds broad-ranging of biological activity [6]. Piperidine-4-one compound has been attained much attention in recent years due to their biological activities and their molecular structures in various drugs [5]. Piperidones are a class of organic compounds consist of piperidine skeleton, that mimic the naturally occurring alkaloids and steroids which have been synthesized in order to study their biological activity and compare with naturally occurring compounds. It has been reported as antimicrobial, antiviral, analgesic, antioxidant and anticancer activities [6-10].

Previously, we reported the bond topological and electrostatic properties of piperidine-4-one compounds by using DFT method [11]. In continuation of our earlier work, herein we report the DFT calculations to study about the molecular structure of 3ECl, 3MCl and 3,5-DMCl using mulliken atomic population, molecular electrostatic potential, frontier molecular orbital, non-linear optical property. Molecular geometries were calculated by density functional theory (DFT) using B3LYP/6-311G (d,p) basis set [12,13]. Adopting the above techniques, the molecular structure, chemical bonding and the reaction mechanisms of three compounds *viz.* (*E*)-1-(2,6-*bis*(4-chlorophenyl)-3-ethyl-piperidine-4-ylidene)-2-phenylhydrazine (3ECl), (*E*)-1-(2,6-*bis*(4-chlorophenyl)-3-methylpiperidine-4-ylidene)-2-phenylhydrazine (3MCl), (*E*)-1-(2,6-*bis*(4-chlorophenyl)-3,5-dimethylpiperidine-4-ylidene)-2-phenylhydrazine (3,5-DMCl), using computational DFT method were investigated.

EXPERIMENTAL

The quantum chemical calculations of three compounds *viz.* (*E*)-1-(2,6-*bis*(4-chlorophenyl)-3-ethyl-piperidine-4-ylidene)-2-phenylhydrazine (3ECl), (*E*)-1-(2,6-*bis*(4-chlorophenyl)-3-methylpiperidine-4-ylidene)-2-phenylhydrazine (3MCl), (*E*)-1-(2,6-*bis*(4-chlorophenyl)-3,5-dimethylpiperidine-4-ylidene)-2-phenylhydrazine (3,5-DMCl) were executed by applying DFT method B3LYP with 6-311G (d,p) basis set using Gaussian 09 software.

Computational studies: The quantum chemical calculation has been performed in Gaussian 09 program package with help of density functional theory (DFT) [14,15]. The structure of molecule was optimized by the density functional theory using hybrid functional B3LYP (Becke′s three-parameter exchange functional [16] combined with Lee-Yang-Parr correlation functional [17] with the 6-31G (d,p) basis set [16]. The optimized parameters performed as vibrational frequency calculation in the DFT to characterize all the stationary points as minima [18]. The functions of calculated frequencies are assisted by the animation option of chemcraft program [19]. The B3LYP method used to evaluate the molecular electrostatic potential of reactive sites of title compounds. The dipole moment (μ), polarizability (α) and hyperpolarizability (β) are calculated by computed value. The HOMO-LUMO energies are predicted by using TD-DFT approach [14]. The Gauss view aid shows the molecular structure of compounds [20]. Mulliken atomic charges predict the charge distribution of each atom present in a molecular systems [21]. The molecular geometry is optimized without any restriction.

RESULTS AND DISCUSSION

Optimized geometry: The optimized molecular structure with the numbering of atoms of substituted piperidine phenyl hydrazine compounds (3ECl, 3MCl and 3,5-DMCl) are shown in Fig. 1. The predicted geometrical parameters such as bond length, bond angle and dihedral angle of 3ECl calculated at B3LYP/6-311G (d,p) level of theory are presented in Tables 1-3.

TABLE-1
OPTIMIZED GEOMETRICAL PARAMETERS OF 3ECl

Atoms	Bond length (Å)	Atoms	Bond length (Å)
C1-C6	1.513	C13-Cl31	1.829
C5-C6	1.522	C13-C12	1.392
C4-C5	1.573	C14-C13	1.399
C1-C2	1.558	C12-H38	1.083
C2-N3	1.47	C14-H39	1.082
N3-C4	1.478	C18-Cl30	1.828
N3-H10	1.017	C18-C19	1.393
C1-H32	1.095	C17-C18	1.392
C1-H33	1.097	C17-H42	1.083
C6-N7	1.298	C19-H43	1.083
N7-N21	1.365	C5-C28	1.541
N21-H45	1.0365	C28-C29	1.538
N21-C22	1.401	C28-H51	1.096
C22-C23	1.408	C28-H52	1.096
C22-C27	1.35	C29-H55	1.093
C27-H50	1.115	C29-H54	1.098
C23-H46	1.087	C29-H53	1.096
C4-C8	1.52		
Atoms	Bond angle (°)	Atoms	Bond angle (°)
C23-C22-C27	119.56	C6-C5-C28	114.23
C22-N21-N7	120.93	C4-C5-C28	112.61
N21-N7-C6	122.1	C11-C8-C15	118.66
C1-C6-C5	114.46	C16-C9-C20	118.79
C6-C5-C4	107.46	C12-C13-C14	121.87
C5-C4-N3	108.84	C17-C18-C19	121.87
C6-C1-C2	109.65	C17-C18-Cl30	119.06
C1-C2-N3	107.75	C19-C18-Cl30	119.08
C2-N3-H10	112.43	C4-N3-H10	112.14
Atoms	Dihedral angle (°)	Atoms	Dihedral angle (°)
C22-N21-N7-C6	179.134	C4-C5-C28-C29	-163.101
N21-N7-C6-C5	178.593	C6-C1-C2-N3	54.065
N7-C6-C5-C4	-120.77	C4-C8-C11-C12	179.719
C4-N3-C2-C1	-59.184	C4-C8-C15-C14	-179.794
C6-C5-C28-C29	73.293	C2-C9-C16-C17	-177.781
C11-C12-C13-Cl31	179.787	C2-C9-C20-C19	177.97
C15-C14-C13-Cl31	-179.858	N3-C4-C5-C28	179.851
C16-C17-C18-Cl30	-179.82	N3-C2-C9-C20	40.708
C20-C19-C18-Cl30	-179.987		

Mulliken atomic charges: Mulliken atomic charge calculation has an important role in the application of quantum chemical calculation to molecular system because of atomic charges affect dipole moment, molecular polarizability, electronic structure and a lot of properties of molecular systems. The charge distributions over the atoms suggest the formation of donor and acceptor pairs involving the charge transferring in the molecule. The Mulliken population analysis in 3,5-DMCl molecule was calculated using B3LYP level with 6-311G (d,p) basis set (Table-4). The Mulliken charge distribution structure of 3,5-DMCl is shown in Fig. 2. The charge distributions of this compound revealed that the carbon atoms attached with hydrogen atoms and C6, C8, C9 and C22 atoms are positively charged and remaining carbon atoms are negatively charged. A 21N has the greater negative charge than the other two nitrogen atoms, as well as all hydrogen atoms have a positive charge. The Mulliken atomic charges shows the N atoms attached with C and H atoms. The 44H and 10H have a high positive charge than the other hydrogen atoms. The 44H and 10H have to be attached with 21N and 7N atoms and these two atoms have the higher positive charge because of electronegativity of N atoms [14]. A 22C atom has more positive charge compared to other C atoms in this compound and it also attached with more electronegative atom 21N. Similarly, more negative charge is carried by the carbon atoms 31C and 28C [15].

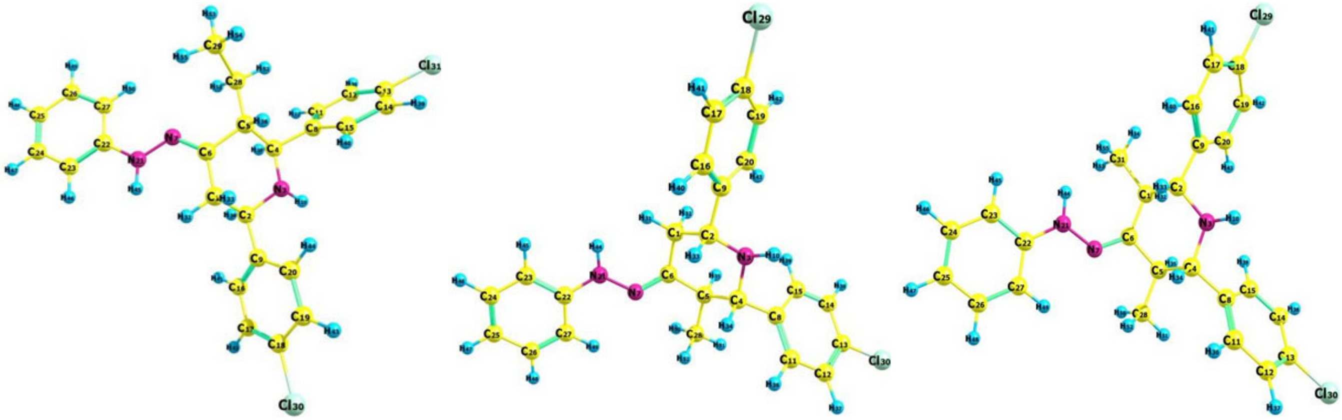

Fig. 1. Optimized geometry of 3ECl, 3MCl and 3,5-DMCl

TABLE-2
OPTIMIZED GEOMETRICAL PARAMETERS OF 3MCl

Atoms	Bond length (Å)	Atoms	Bond length (Å)
C23-C22	1.407	C8-C11	1.404
C22-C27	1.406	C8-C15	1.399
C22-N21	1.402	C13-C14	1.393
N21-H44	1.013	C13-C12	1.392
N21-N7	1.364	C13-Cl30	1.829
N7-C6	1.298	C2-C9	1.519
C6-C1	1.514	C9-C20	1.406
C6-C5	1.521	C9-C16	1.404
C1-C2	1.556	C18-C17	1.392
C2-N3	1.47	C18-C19	1.393
N3-C4	1.478	C18-Cl29	1.828
C4-C5	1.569	C5-C28	1.533
N3-H10	1.017	C28-H50	1.093
C1-H31	1.095	C28-H51	1.094
C4-C8	1.519	C28-H52	1.096
Atoms	**Bond angle (Å)**	**Atoms**	**Bond angle (Å)**
C23-C22-C27	119.6	C5-C28-H52	111.1
C24-C25-C26	119.1	C5-C28-C51	110.65
C23-C22-N21	118.64	C5-C4-N3	108.96
C23-N21-H44	117.98	C4-N3-C2	116
C22-N21-N1	120.81	C1-C2-N3	107.89
N7-N21-H44	121.16	C16-C9-C2	120.38
C6-N7-N21	122.13	C2-C9-C20	120.81
C2-C1-C6	110.36	C16-C9-C20	118.78
C4-C5-C6	109.14	C17-C18-Cl29	119.1
C6-C5-C28	113.39	C19-C18-Cl29	119.07
C5-C28-H50	110.43	C17-C18-C19	121.87
Atoms	**Torsion angle (°)**	**Atoms**	**Torsion angle (°)**
C27-C22-N21-N7	1.62	C2-C9-C16-C17	-177.959
C23-C22-N21-N7	-178.508	C9-C16-C17-C18	-0.233
C22-N21-N7-C6	-179.789	C16-C17-C18-Cl29	-179.821
N21-N7-C6-C1	1.582	C20-C19-C18-Cl29	-180
N7-C6-C1-C2	125.93	C1-C6-C5-C28	177.975
N7-C6-C5-C4	-127.29	N3-C4-C5-C28	-178.506
C1-C2-N3-C4	-60.452	C4-C8-C11-C12	179.255
C6-C1-C2-N3	53.531	C4-C8-C15-C14	-179.363
C6-C5-C4-N3	-52.026	C15-C14-C13-Cl30	-179.892

TABLE-3
OPTIMIZED GEOMETRICAL PARAMETERS OF 3,5-DMCl

Atoms	Bond length (Å)	Atoms	Bond length (Å)
C23-C22	1.408	C3-H53	1.095
C22-C27	1.406	C3-H54	1.094
C22-N21	1.403	C3-H55	1.098
N21-H44	1.009	C5-C28	1.532
N21-N7	1.362	C28-H50	1.093
N7-C6	1.297	C28-H51	1.094
C6-C1	1.517	C28-H52	1.095
C6-C5	1.528	C18-Cl29	1.828
C4-C5	1.52	C18-C19	1.394
C4-N3	1.475	C18-C17	1.392
C2-N3	1.472	C13-Cl30	1.829
N3-H10	1.017	C13-C12	1.392
C1-C2	1.573	C13-C14	1.394
C1-C3	1.54		
Atoms	**Bond angle (°)**	**Atoms**	**Bond angle (°)**
C23-C22-C27	119.56	N3-C4-C5	108.8
C23-C22-N21	118.51	C4-N3-H10	112.42
C22-N21-N7	120.19	C2-N3-H10	112.42
N21-N7-C6	125.73	C12-C13-Cl30	119.08
H44-N21-N7	121.88	C14-C13-Cl30	119.04
N7-C6-C1	131.47	C14-C13-C12	121.88
N7-C6-C5	115.91	C15-C8-C11	118.66
C6-C5-C4	107.74	C16-C9-C20	118.66
C6-C1-C2	107.74	C17-C18-Cl29	119.08
C1-C2-N3	108.04	C19-C18-Cl29	119.07
C2-N3-C4	117.67	C17-C18-C11	121.85
Atoms	**Torsion angle (°)**	**Atoms**	**Torsion angle (°)**
C23-C22-N21-N7	179.38	C6-C1-C2-N3	56.101
C27-C22-N21-N7	-0.52	C1-C2-C9-C16	106.111
C22-N21-N7-C6	179.219	C1-C2-C9-C20	-73.509
N21-N7-C6-C1	1.442	C16-C17-C18-Cl29	-179.894
N7-C6-C1-C2	113.587	C20-C19-C18-Cl29	179.91
N7-C6-C1-C31	-14.661	C4-C8-C15-C14	-178.931
N7-C6-C5-C28	9.313	C4-C8-C11-C12	178.879
C6-C5-C4-N3	-53.889	C15-C14-C13-Cl30	-179.905
		C11-C12-C13-Cl30	179.856

Molecular electrostatic potential (MEP): The molecular electrostatic potential is related to the electronic density and also useful descriptor for determining sites for electrophilic and nucleophilic reactions as well as hydrogen-bonding interactions [14,22-24]. Molecular electrostatic potential surface for 3ECl, 3MCl, 3,5-DMCl are obtained by DFT/B3LYP using 6-311G (d,p) basis set. The shapes, sizes, charge densities, delocalization and reactive sites were determined for 3ECl, 3MCl, 3,5-DMCl [25]. The charge distribution of molecule is

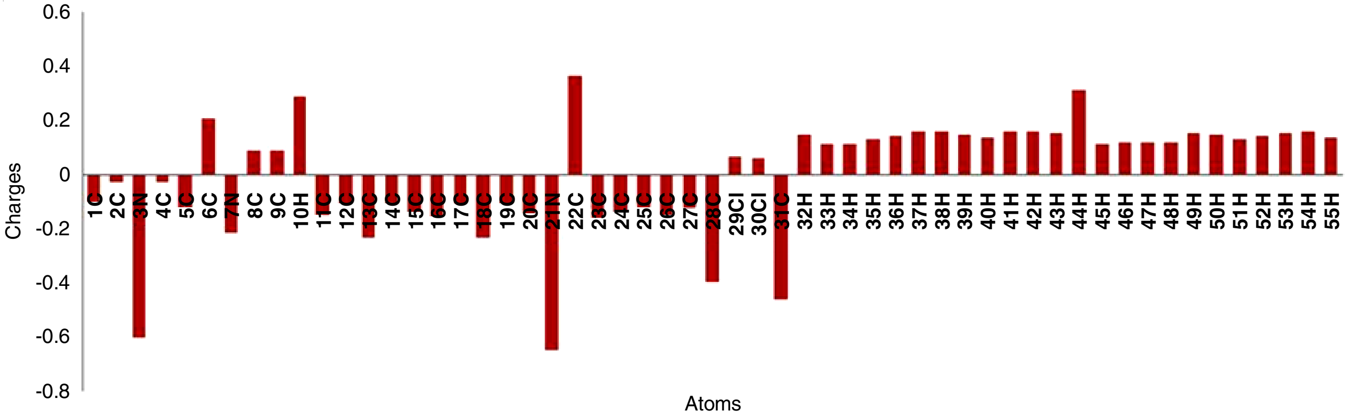

Fig. 2. Mulliken atomic charge distribution of 3,5-DMCl

TABLE-4
MULLIKEN POPULATION ANALYSIS OF 3,5-DMCl

Atoms	Charges	Atoms	Charges
1C	-0.0948	29Cl	0.0659
2 C	-0.0287	30Cl	0.0608
3N	-0.6023	31C	-0.4588
4C	-0.027	32H	0.1504
5C	-0.1222	33H	0.1131
6C	0.2051	34H	0.1154
7N	-0.2115	35H	0.1343
8C	0.0924	36H	0.1404
9C	0.0911	37H	0.1592
10H	0.2893	38H	0.1582
11C	-0.1515	39H	0.1509
12 C	-0.1025	40H	0.1384
13C	-0.2293	41H	0.1606
14C	-0.1026	42H	0.1609
15C	-0.1369	43H	0.1559
16C	-0.1549	44H	0.3131
17C	-0.1022	45H	0.112
18C	-0.2304	46H	0.1211
19C	-0.1025	47H	0.1182
20C	-0.1391	48H	0.1219
21N	-0.6462	49H	0.1545
22C	0.3638	50H	0.1474
23C	-0.1641	51H	0.1337
24C	-0.1393	52H	0.1412
25C	-0.1184	53H	0.1557
26C	-0.1449	54H	0.1628
27C	-0.1204	55H	0.1371
28C	-0.3941	–	–

arranged in a three dimensional orientation. The different values of electrostatic potential at the surface are represented by different colours: red or yellow represents regions of most electronegative electrostatic potential. Blue represents regions of the most positive electrostatic potential and green represents region of zero potential. Potential increases in the order of red < orange < yellow < green < blue. Fig. 3 shows that in all molecules, the regions reveals the positive potentials are localized over the vicinity of hydrogen atoms and the regions reveals the negative potentials are localized over the phenyl ring and two chlorine atom. Compound 3,5-DMCl has a highly rich in negative and positive charge on phenyl ring and hydrogen atoms so these two sites are chemically active.

Frontier molecular orbitals: The frontier molecular orbital can offer a reasonable qualitative prediction of the excitation properties and the ability of electron transport [14,26,27]. The electronic absorption basically means the transition from the ground to the excited state and mainly described by electron transition from the highest occupied molecular orbital (HOMO) to the lowest unoccupied molecular orbital (LUMO) [16]. So, 3,5-DMCl molecule has chemical stability and chemical reactivity. The value of energy separation between the HOMO and LUMO were calculated by using B3LYP/6-311 G (d,p). The red represents the positive electron and green represents the negative electron. In HOMO electrons are localized over the ring A and LUMO the electrons are localized over the ring B and C (Fig. 4). Three compounds 3ECl, 3MCl, 3,5-DMCl have an energy gap of 4.466

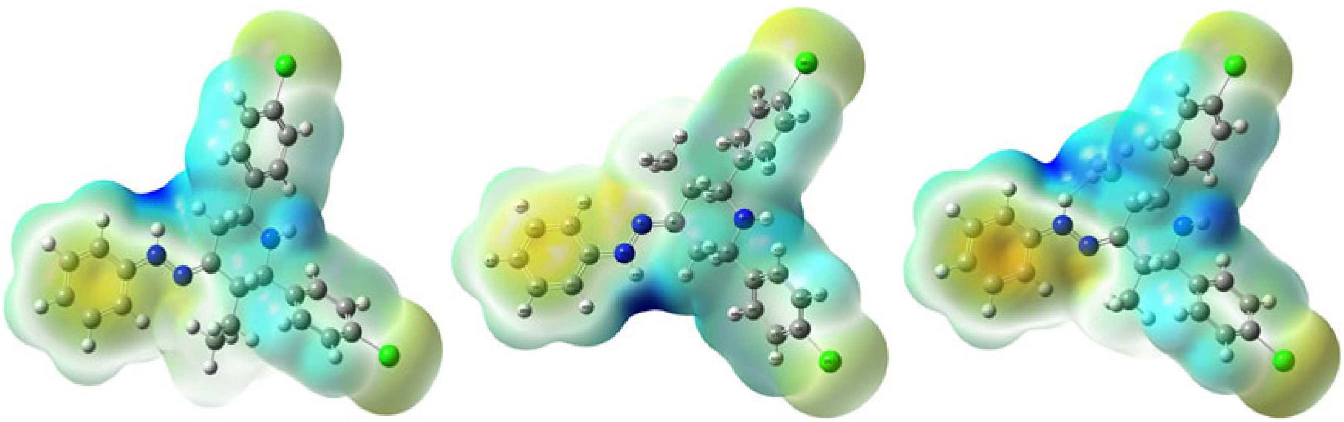

Fig. 3. Molecular electrostatic potential of 3ECl, 3MCl and 3,5-DMCl

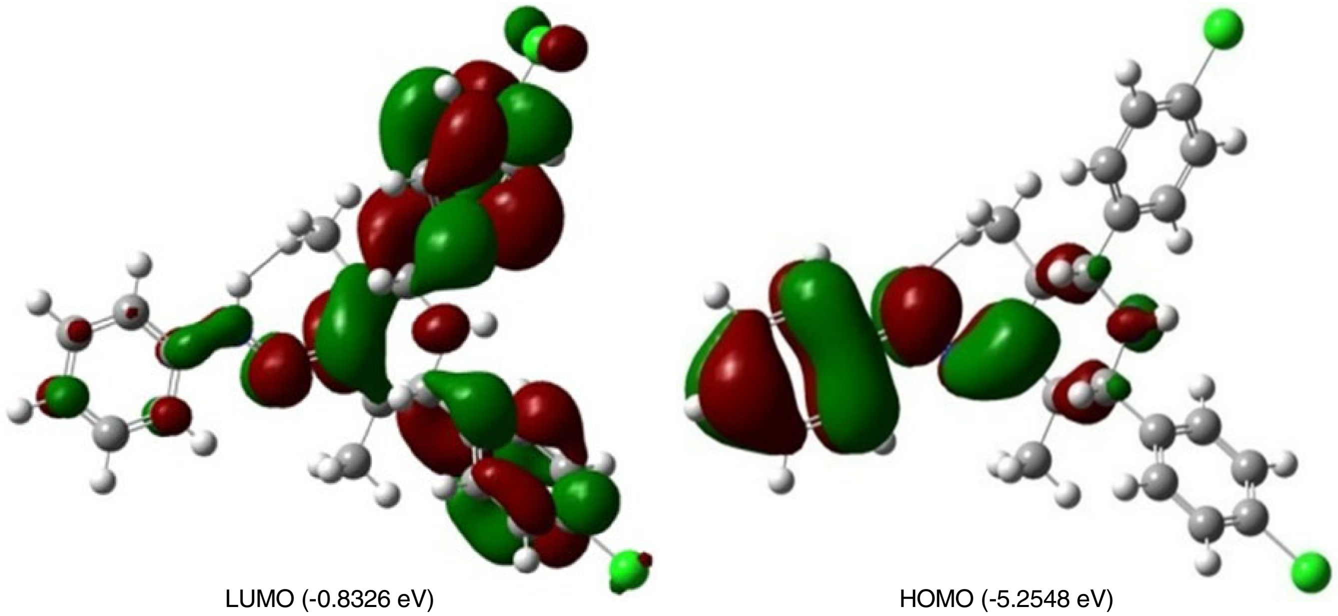
LUMO (-0.8326 eV) HOMO (-5.2548 eV)

Fig. 4. Frontier molecular orbital of 3,5-DMCl

eV, 4.4841 eV and 4.418 eV, respectively. So, 3,5-DMCl molecule has highest chemical stability and chemical reactivity.

Global reactivity descriptors: The chemical reactivity and site selectivity determination of molecules was done by Koopman′s theorem. The compound which have the lowest energy gap is the 3,5-DMCl (ΔE_{gap} = 4.418 eV). The lower energy gap allows it to be the softest molecule. The compound have the highest energy gap is 3MCl (ΔE_{gap} = 4.4841 eV). The compound has the highest HOMO energy is the compound 3,5-DMCl (E_{HOMO} = -5.255 eV) and higher energy permit it to be the best electron donor. The compound that has the lowest LUMO energy is the compound 3,5-DMCl (E_{LUMO} = -0.833eV), which indicates that it can be the best electron acceptor (Table-5).

TABLE-5
CALCULATED ENERGY VALUES OF 3ECl, 3MCl, 3,5-DMCl

Compounds	3ECl	3MCl	3,5-DMCl
E_{LUMO}	-0.8264	-0.8019	-0.833
E_{HOMO}	-5.2932	-5.286	-5.255
Energy gap (E_L-E_H)	4.4660	4.4841	4.418
Ionization potential (I)	5.2932	5.2860	5.255
Affinity (A)	0.8264	0.8019	0.833
Electronegativity (χ)	3.0598	3.0439	3.0437
Chemical potential (μ)	-3.0598	-3.0439	-3.044
Global hardness (η)	2.2334	2.24205	2.2111
Global softness (S)	1.1167	1.12102	1.1055
Electrophilic index (ω)	2.0959	2.0663	2.095

Compound 3,5-DMCl has lowest value of potential ionization (I = 5.2932 eV), so acts as a better electron donor, while compound 3,5-DMCl has the largest value of affinity (A = 0.833 eV), henceforth act as a better electron acceptor. The chemical reactivity varies with the structural molecules. Chemical hardness (softness) value of compound 3,5-DMCl (η = 2.2111 eV, S = 1.1055) is lesser (greater) among all the molecules. Thus, compound 3,5-DMCl is found to be more reactive among all the studied compounds. Compound 3ECl possesses higher electronegativity value (χ = 3.0598 eV) than all compounds, so it is the leading electron acceptor. The value of electrophilic index (ω) for compound 3ECl (ω = 2.0959 eV) denotes that it is the stronger electrophiles than all compounds. The compound 3,5-DMCl has the lesser frontier energy gap so, it is more polarizable and associated with a high chemical reactivity, low kinetic stability (Table-5) and also termed as soft molecule [28].

Non-linear optical (NLO) properties: Density functional theory has been used as an effective method to investigate the organic non-linear optical (NLO) materials. It provides key functions of frequency shifting, optical modulation, optical logic, optical switching and optical memories for the emerging technologies in areas such as telecommunication, signal processing and optical interconnections [20,29-33]. The polarizability (α), hyperpolarizability (β) and the electric dipole moment (μ) of title compounds are calculated by finite field method using B3LYP/6-311G (d,p) basis set available in Gaussian 09 package. The polarizability and hyperpolarizability tensors (α_{xx}, α_{xy}, α_{yy}, α_{xz}, α_{yz}, α_{zz} and β_{xxx}, β_{xxy}, β_{xyy}, β_{yyy}, β_{xxz}, β_{xyz}, β_{yyz}, β_{xzz}, β_{yzz}, β_{zzz}) can be obtained by a frequency job output file of Gaussian 09.

$$\mu = \left(\mu_x^2 + \mu_y^2 + \mu_z^2\right)^{1/2}$$

$$\alpha_0 = \frac{1}{3}\left(\alpha_{xx} + \alpha_{yy} + \alpha_{zz}\right)$$

$$\beta_0 = \Big[(\beta_{xxx} + \beta_{xyy} + \beta_{xzz})^2 + (\beta_{yyy} + \beta_{xxy} + \beta_{yzz})^2 + (\beta_{zzz} + \beta_{xxz} + \beta_{yyz})^2\Big]^{1/2}$$

However, α and β values of Gaussian output are in atomic units (a.u.) so they have been converted into electronic units (esu) (α: 1 a.u. = 0.1482 × 10^{-24} esu, β: 1 a.u. = 8.6393 × 10^{-33} esu). The complete equations for calculating the magnitude of total static dipole moment (μ), mean polarizability total (α_{tot}), anisotropy of polarizability (α) and the mean first hyperpolarizability (β_o) can be calculated using the equations, respectively [34]. Urea is one of the photolytical molecules used in the study of the NLO properties of the molecular systems. Therefore, it was used frequently as a threshold value for comparative purposes. The calculated values of dipole moment (μ) for the compounds were found to be -1.1896, -0.9872 and 2.5045, respectively. The 3,5-DMCl value is two times higher than to the value of urea (μ = 1.3732D). The values of hyperpolarizability (β_o) are -1.6169×10^{-30}, -1.5538×10^{-30} and 1.6475×10^{-30} esu calculated. The 3,5-DMCl value is higher than that of urea 0.3728×10^{-30} esu, while the values of polarizability (α_o) are found to be -2.9974×10^{-23}, -2.9005×10^{-23} and -2.9964×10^{-23} esu, respectively for 3ECl, 3MCl, 3,5-DMCl molecules (Table-6).

TABLE-6
NON-LINEAR OPTICAL PARAMETERS OF 3ECl, 3MCl, 3,5-DMCl

Parameters	3ECl	3MCl	3,5-DMCl
μ_x	-1.654	-1.5861	-1.7377
μ_y	0.9079	0.8765	1.7243
μ_z	0.8497	0.9126	0.529
μ	-1.1896	-0.9872	2.5045
α_{xx}	-206.9044	-200.7135	-208.7175
α_{xy}	-1.9219	-1.2651	-3.4474
α_{yy}	-212.9405	-206.8203	-211.37707
α_{xz}	-4.0931	-2.9987	-5.1329
α_{yz}	-1.919	-2.4933	-2.0863
α_{zz}	-186.9216	-179.6151	-186.4767
α_0	-202.2555	-195.7163	-202.1904
α_0 (esu)	-2.9974×10^{-23}	-2.9005×10^{-23}	-2.9964×10^{-23}
β_{xxx}	-124.3148	-133.7215	-70.4879
β_{xxy}	93.9662	97.7847	-62.1451
β_{xyy}	-101.41	42.222	-157.6246
β_{yyy}	-148.965	-153.2058	-62.1451
β_{xxz}	-10.0301	-6.8109	-11.8934
β_{xyz}	-13.6343	-18.9345	-6.9908
β_{yyz}	38.0385	35.6918	34.1488
β_{xzz}	42.4164	42.222	38.652
β_{yzz}	8.0519	12.2455	6.5934
β_{yzz}	-0.1177	-0.179	-1.9657
β_0	-187.1579	-179.8582	190.6983
β_0 (esu)	-1.6169×10^{-30}	-1.5538×10^{-30}	1.6475×10^{-30}

Conclusion

Three substituted piperidine phenyl hydrazines 3ECl, 3MCl and 3,5-DMCl were theoretically studied using density functional theory employing Becke's three parameter hybrid exchange functional with Lee-Yang-Parr (B3LYP) co-relational functional involving 6-311G (d,p) basis set. The optimized molecular parameters such as bond length, bond angle were analyzed by DFT method. The molecular electrostatic potential map of studied compounds, positive region is mainly localized over the hydrogen atom and negative region localized over the phenyl ring and Cl atoms. The FMO analysis identifies the presence of delocalized electron density within the molecule and energy gap calculated. Insight into the global reactivity properties has been obtained by analysis of frontier molecular orbital.

CONFLICT OF INTEREST

The authors declare that there is no conflict of interests regarding the publication of this article.

REFERENCES

1. R. Rohs, I. Bloch, H. Sklener and Z. Shakked, *Nucleic Acids Res.*, **33**, 7048 (2005); https://doi.org/10.1093/nar/gki1008.
2. I.A. Guedes, C.S. de Magalhães and L.E. Dardenne, *Biophys. Rev.*, **6**, 75 (2014); https://doi.org/10.1007/s12551-013-0130-2.
3. B.P. Lanyon, J.D. Whitfield, G.G. Gillett, M.E. Goggin, M.P. Almeida, I. Kassal, J.D. Biamonte, M. Mohseni, B.J. Powell, M. Barbieri, A. Aspuru-Guzik and A.G. White, *Nat. Chem.*, **2**, 106 (2010); https://doi.org/10.1038/nchem.483.
4. D.A.H. Hanaor, M.H.N. Assadi, S. Li, A. Yu and C.C. Sorrell, *Comput. Mech.*, **50**, 185 (2012); https://doi.org/10.1007/s00466-012-0728-4.
5. C. Ramalingam, Y.T. Park and S. Kabilan, *Eur. J. Med. Chem.*, **41**, 683 (2006); https://doi.org/10.1016/j.ejmech.2006.02.005.
6. S. Balasubramanian, G. Aridoss, P. Parthiban, C. Ramalingan and S. Kabilan, *Biol. Pharm.*, **29**, 125 (2006); https://doi.org/10.1248/bpb.29.125.
7. A. Manimekalai, J. Jayabharathi, L. Rufina and R. Mahendran, *Indian J. Chem.*, **42B**, 2074 (2003).
8. C.R. Noller and V. Baliah, *J. Am. Chem. Soc.*, **70**, 3853 (1948); https://doi.org/10.1021/ja01191a092.
9. P.S. Watson, B. Jiang and B. Scott, *Org. Lett.*, **2**, 3679 (2000); https://doi.org/10.1021/ol006589o.
10. N. Rameshkumar, A. Veena, R. Ilavarasan, P. Shanmugapandiyan, M. Adiraj and S.K. Sridhar, *Biol. Pharm. Bull.*, **26**, 188 (2003); https://doi.org/10.1248/bpb.26.188.
11. K. Ajay Kumar, G. Pavithra, N. Renuka and G. Vasanth Kumar, *Int. Res. J. Pharm. Appl. Sci*., **2**, 145 (2012).
12. S. Guidara, H. Feki and Y. Abid, *J. Mol. Struct.*, **1080**, 176 (2015); https://doi.org/10.1016/j.molstruc.2014.09.084.
13. K. Bhavani, S. Renuga, S. Muthu and K. Sankaranarayanan, *Spectrochim. Acta A Mol. Biomol. Spectrosc.*, **136**, 1260 (2015); https://doi.org/10.1016/j.saa.2014.10.012.
14. A.D. Becke, *Physical Review A*, **38**, 3098 (1988); https://doi.org/10.1103/PhysRevA.38.3098.
15. C. Lee, W. Yang and R.G. Parr, *Phys. Rev. B Condens. Matter*, **37**, 785 (1988); https://doi.org/10.1103/PhysRevB.37.785.
16. H. Saleem, S. Subashchandrabose, N. Ramesh Babu and M. Syed Ali Padusha, *Spectrochim. Acta A Mol. Biomol. Spectrosc.*, **143**, 230 (2015); https://doi.org/10.1016/j.saa.2015.02.016.
17. G.A. Zhurko and D.A. Zhurko, Chemcraft Program, Academic version 1.5 (2004).
18. R.P. Singh, R. kant, K. Singh, S. Sharma and A. Sethi, *J. Mol. Struct.*, **1095**, 125 (2015); https://doi.org/10.1016/j.molstruc.2015.04.018.
19. M. Rajkumar, P. Muthuraja, M. Dhandapani and A. Chandramohan, *J. Mol. Struct.*, **1153**, 192 (2018); https://doi.org/10.1016/j.molstruc.2017.10.013.
20. E. Scrocco and J. Tomasi, New Concepts II, Springer, Berlin-Heidelberg, p. 95 (1973).
21. F.J. Luque, J.M. López and M. Orozco, *Theor. Chem. Acc.*, **103**, 343 (2000); https://doi.org/10.1007/s002149900013.
22. N. Okulik and A.H. Jubert, *Internet Electr. J. Mol. Design*, **4**, 17 (2005).
23. M.S. Alam and D.U. Lee, *Spectrochim. Acta A Mol. Biomol. Spectrosc.*, **145**, 563 (2015); https://doi.org/10.1016/j.saa.2015.03.071.
24. M. Belletête, J.F. Morin, M. Leclerc and G. Durocher, *J. Phys. Chem. A*, **109**, 6953 (2005); https://doi.org/10.1021/jp051349h.
25. D. Zhenming, S. Heping, L. Yufang, L. Diansheng and L. Bo, *Spectrochim. Acta A Mol. Biomol. Spectrosc.*, **78**, 1143 (2011); https://doi.org/10.1016/j.saa.2010.12.067.
26. A. Tahar, B. Amel and V. Didier, *Int. J. Adv. Res. Sci. Eng. Technol.*, **5**, 5504 (2018).
27. N.B. Singh, O.P. Singh, N.P. Singh, N. Singh, Y.P. Singh and N.B. Singh, *Prog. Cryst. Growth Charact. Mater.*, **44**, 169 (2002); https://doi.org/10.1016/S0960-8974(02)00014-1.

28. C. Andraud, T. Brotin, C. Garcia, F. Pelle, P. Goldner, B. Bigot and A. Collet, *J. Am. Chem. Soc.*, **116**, 2094 (1994); https://doi.org/10.1021/ja00084a055.

29. V.M. Geskin, C. Lambert and J.L. Brédas, *J. Am. Chem. Soc.*, **125**, 15651 (2003); https://doi.org/10.1021/ja035862p.

30. M. Nakano, H. Fujita, M. Takahata and K. Yamaguchi, *J. Am. Chem. Soc.*, **124**, 9648 (2002); https://doi.org/10.1021/ja0115969.

31. D. Sajan, H. Joe, V.S. Jayakumar and J. Zaleski, *J. Mol. Struct.*, **785**, 43 (2006); https://doi.org/10.1016/j.molstruc.2005.09.041.

32. Y. Sun, X. Chen, L. Sun, X. Guo and W. Lu, *Chem. Phys. Lett.*, **381**, 397 (2003); https://doi.org/10.1016/j.cplett.2003.09.115.

33. O. Christiansen, J. Gauss and J.F. Stanton, *Chem. Phys. Lett.*, **305**, 147 (1999); https://doi.org/10.1016/S0009-2614(99)00358-9.

34. N. Issaoui, H. Ghalla, S. Muthu, H.T. Flakus and B. Oujia, *Spectrochim. Acta A Mol. Biomol. Spectrosc.*, **136**, 1227 (2015); https://doi.org/10.1016/j.saa.2014.10.008.